Proceedings of Intelligent Systems and Manufacturing: Tech. Conf. on Microrobotics and Microsystem Fabrication, Pittsburgh, 16-17 Oct. 1997, pp. 86-95.

Active hand-held instrument for error compensation in microsurgery

Cameron N. Riviere and Pradeep K. Khosla
The Robotics Institute, Carnegie Mellon University, Pittsburgh, PA 15213-3891 USA

ABSTRACT

Physiological hand tremor and other manual positioning errors limit precision in microsurgical procedures. Our research has involved development of adaptive algorithms and neural network methods for real-time compensation of such errors. This paper presents a novel design for an active hand-held microsurgical instrument to implement these algorithms, particularly during vitreoretinal microsurgery. The basic vitreoretinal instrument consists of a handle fitted with a narrow intraocular shaft to provide access to the interior of the eye. In our design, the instrument handle incorporates six-degree-of-freedom inertial sensing to determine the three-dimensional position of the instrument tip. The intraocular shaft is attached to the instrument handle via a miniature parallel manipulator with three degrees of freedom, controlled by three piezoelectric elements. The manipulator actuates the intraocular shaft in pitch, yaw, and axial extension, allowing the system to perform active compensation of errors in the position of the tip of the intraocular shaft. The paper includes the formulation of the inverse kinematics of the instrument in a manner suitable for online computation. A discussion of practical design considerations and the methods and results of preliminary experiments are also presented.

Keywords: microsurgery, tremor, active noise control, mechatronics, instrument design

1. INTRODUCTION

Microsurgical practice has begun to encounter the limits of human precision. This is especially true in vitreoretinal and other ophthalmological procedures. These limits arise due to involuntary and inadvertent movements of the hand, which create a noise or error component in hand motion, placing a lower bound on the size of voluntary motion that can be generated. The most familiar source of undesired hand motion is physiological tremor, which is an approximately rhythmic, roughly sinusoidal involuntary component inherent in all human motion[1]. Low-frequency errors, or drift, are also present in hand motion, and are often larger than tremor[2]. Irregular high-frequency motion, or jerk, can also occur[3]. The results are that some procedures are less precise than is desired, and some desired procedures cannot be done at all[4]. Several examples of these may be found in a fine review by Charles[4]. Microsurgical practice would therefore benefit greatly from systems that enhance accuracy by compensating position error.

Most attempts to develop such systems have involved teleoperative approaches, such as those of Hunter *et al.*[5] and Schenker *et al.*[3]. Telerobotic systems have the potential not only to filter out involuntary components from the input received from the master interface, but also to perform motion scaling (i.e., mapping large hand movements to small slave manipulator movements) and force feedback[3], and are of course the only option for remote surgery. However, there is resistance among eye surgeons to robotic systems[6], perhaps largely because of their unfamiliar nature and feel for the surgeon. Contributing to this unnatural feel is the time delay sometimes encountered in telerobotic systems[7]. The high cost of such systems is another strong drawback, particularly in the current economy of health care.

If the necessary sensing and actuation can be incorporated within the confines of a hand-held surgical instrument, it is possible to implement error canceling (though not motion scaling or force feedback). This can be done by estimating the involuntary component of motion, then generating an opposing motion of the tip of the instrument, actively compensating or subtracting the involuntary portion from the total motion. Such a system requires real-time estimation of voluntary motion, as a compensating motion with time delay will be ineffective, and the overall motion of the instrument by the surgeon's hand cannot be delayed by the system. However, this points out one benefit of such a system, which is that real-time correspondence of the surgeon's input and instrument output is guaranteed, both being aboard the same instrument. This

Author information:
C.N.R.: cam.riviere@cs.cmu.edu; http://www.cs.cmu.edu/~camr
P.K.K.: pkk@ices.cmu.edu; http://www.cs.cmu.edu/afs/cs/project/chimera/www/people/pradeep.html

active compensation approach requires less hardware, and can therefore be implemented at lower cost than a telerobotic system. Furthermore, such a system maximizes transparency to the surgeon, since the technique is implemented within the familiar hand-held instrument itself, and thereby maximizes the likelihood of psychological acceptance.

Active error compensation within a hand-held microsurgical instrument therefore holds much potential for improved precision, and its concomitant benefits to patients, at low cost. This paper describes our ongoing work in development of an active hand-held instrument for compensation of physiological tremor and other position errors in vitreoretinal microsurgery. We discuss the basic design of the instrument, and present the inverse kinematics of the tip manipulator in a form amenable to online computation. We then present the methods and results of preliminary experiments in active error compensation.

2. DESIGN

The typical vitreoretinal microsurgical instrument may be likened to a standard writing pen. It is roughly the diameter of a pen. The largest instruments are also about the length of a pen, the shortest roughly half that. The largest part of the instrument consists of a handle for the hand of the surgeon. Many handles are roughly cylindrical, but recent ergonomic designs include a narrowing at the center of mass, where the instrument is gripped, to aid in holding the instrument with minimal force[4]. Protruding from the tip of the handle is the intraocular shaft. This is a narrow tube, approximately 1 mm in diameter, and typically 2-3 cm long. Through it passes a narrow solid shaft with an end-effector, which may be a forceps, scissor, or other tool. The tool is actuated by retraction of the inner shaft, which causes the end-effector to contact the circular mouth of the tube, thus, e.g., closing the forceps. Traditionally, actuation is accomplished by pressing a button located on the handle. However, the pressing of the button causes an unwanted motion artifact of the tip of the instrument. Rader *et al.*[8] have therefore developed a remote-cam-actuated (RCA) surgical handle in which actuation can be accomplished by the surgeon's other hand, by a foot, or by another person. This handle has reduced the actuation artifact to the level of physiological tremor[8]. Access to the eye is gained by making a sclerotomy, or a small hole in the sclera, through which the intraocular shaft is inserted.

In order to perform active error compensation in a hand-held microsurgical instrument, it is necessary to sense the instrument motion, distinguish desired from undesired motion while avoiding time delay, and then to cause an instrument tip displacement equal and opposite to the undesired motion. This deflection requires an instrument tip manipulator and actuators, and the entire system requires a source of power. A control system is necessary to receive the sensory information, perform the signal filtering, and issue the appropriate command to drive the tip manipulator to the desired position. A computer is needed to perform the signal processing and control functions.

The essential on-board components for such a hand-held instrument are sensing and actuation. Ideally, the instrument would be a true mechatronic device, incorporating its own control computer and power supply, but this is a long-term goal, unattainable with current hardware. In the near term, these functions can be accomplished using a standard desktop computer and power supply connected to the instrument. However, the manipulator, and therefore likewise the actuators, must be part of the instrument itself.

Consideration of the sensing options will show that sensing is best located aboard the instrument as well. There are several possibilities for sensing. The object is to sense the position of the instrument tip. Sensors that require contact or close proximity to the tip are ill suited to the application, due to the impossibility of placing such systems inside the eye, where the instrument tip will be during surgery. Remote sensors do not suffer from this drawback. However, many remote designs are difficult to implement in the cluttered operating room. For example, visual techniques may be impractical due to the likelihood that other objects in the surgical field will obstruct the view of the instrument. Magnetic sensing techniques are problematic due to the large amount of stainless steel that must be used in the operating room, and indeed, in the active instrument itself. Remote sensing techniques would also require development of a mapping from the global reference frame of the fixed sensor to the local frame of the moving instrument. The best sensing approach is therefore one that is aboard the instrument, and requires no contact with fixed objects; thus avoiding the problems encountered with other methods. However, this places a severe volume restriction on the sensor, which must fit within the handle of the instrument.

Inertial sensing offers a solution to this problem. Inertial sensors, such as accelerometers and rate gyros, require neither contact nor maintenance of a line of sight with any fixed object. Furthermore, the recent development of microelectromechanical systems (MEMS) has provided accelerometers that will fit within the instrument handle. Accelerometers have a reputation for noisiness, leading to accumulation of error in cases such as this, where the sensed acceleration will be integrated twice to obtain a position signal. Two factors mitigate this drawback, however. MEMS technology has allowed manufacturers to greatly reduce the noise floor of accelerometers, largely due to the small masses

involved. Secondly, relative, rather than absolute, positioning is of importance. The error modeling techniques we have developed have a generally highpass nature, i.e., noise at low frequencies, such as those where slowly accumulating sensor error would be expected, have little effect on the canceling performance.

The instrument therefore incorporates three ADXL05 accelerometers (Analog Devices, Inc., Norwood, Mass.). These are manufactured in TO-100 cans, cylinders of roughly 5 mm height and 9 mm diameter. Research into MEMS-based rate gyros is ongoing at several centers, but no devices are currently commercially available. In the interim, therefore, our prototype incorporates only three-degree-of-freedom (3-dof) sensing of translation. MEMS-based rotation sensors will be incorporated as soon as they are available, for full 6-dof sensing capability.

The motion of importance in surgery is that of the tip of the instrument. Position is important, orientation less so. It is therefore desired to determine the original manual motion of the instrument tip in three dimensions (3-D) and then to deflect the tip in 3-D to compensate position error. With the intraocular probe protruding from the instrument handle, positioning in the two transverse dimensions (x and y) can be accomplished by appropriate rotation of the shaft about its base, while positioning axially (z) can be done by axial translation of the entire shaft. The intraocular shaft manipulator has therefore been designed as shown in Figure 1. A parallel manipulator design was chosen because of its greater stiffness and accuracy as compared to a serial mechanism[9]. An equilateral triangular plate serves as the base for the intraocular shaft. This plate is mounted at its three vertices to extensible actuators which may be thought of as "table legs" supporting the upper triangle. The upper plate is attached at the same three points to a thin, flexible plastic ring. This ring is also attached at three points, arranged in an equilateral triangular pattern rotated 60˚ from the plate attachments, to rigid mounts that affix it to the base, which is the end of the instrument handle. The actuators also attach to the base in an equilateral triangular pattern, so the base may also be considered to form a triangle for purposes of manipulator analysis. The flexible annulus provides stiffness against unwanted motion in the three degrees of freedom not being actuated, namely, translation in x and y, and rotation about z, while still allowing motion in the three driven degrees of freedom.

Within the small workspace for which this manipulator is intended, the constraints imposed by the flexible annulus make its kinematics essentially equivalent to those of the three-degree-of-freedom (3-dof) parallel manipulator of Lee and Shah[9]. The Lee and Shah actuator has ball joints at the upper ends of the actuators, and pin joints at the lower ends. The orientation of the pin joints constrains each actuator to move in the plane defined by the ω axis and the line from the lower centroid to its respective lower vertex. For kinematic analysis, an orthonormal base frame, $\xi\psi\omega$, is attached to the centroid of the lower triangle, or base. The frame xyz is attached to the centroid of the upper plate, and in its neutral position has the same orientation as $\xi\psi\omega$. The point (x_c, y_c, z_c) is the position of the upper centroid in the reference frame of the base. The initial length of the actuators determines the initial value of z_c, or z_{c_0}. The diameter of the entire manipulator is approximately 15 mm, considering the expected final diameter of 6 mm for each actuator. The intraocular shaft length is l=30 mm. The value r is the distance from centroid to vertex of the upper triangle. The value R is the distance from centroid to vertex of the triangle formed by the lower attachment points of the three actuators. Here, each of the two values is equal to 4.9 mm, thus $\rho = r/R = 1$.

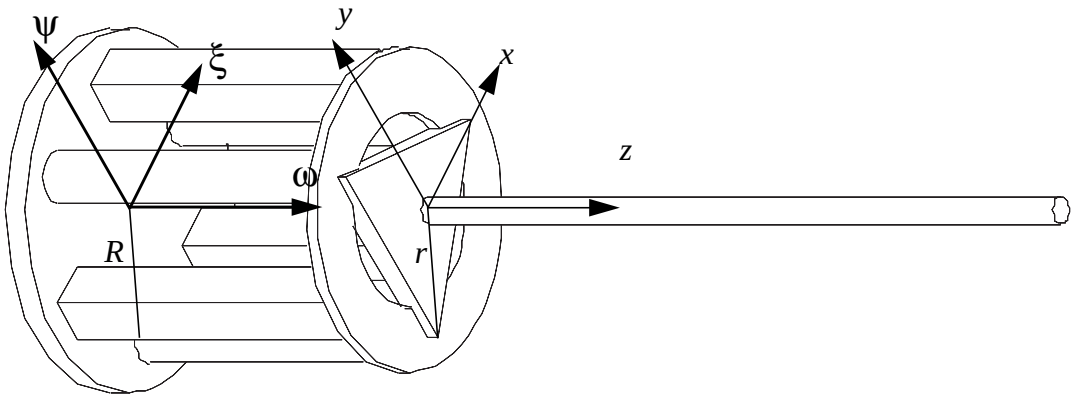

Figure 1. The minimanipulator for the instrument tip. The intraocular shaft is shown pointing toward the right. The three fixed mounts for the flexible ring are represented by rectangular prisms, and the three actuators by cylinders. The orthonormal frame $\xi\psi\omega$ is at the centroid of the lower plate, and the frame xyz at the centroid of the upper plate. R and r are the distances from centroid to actuator on the lower and upper plates, respectively.

Suitable actuators for the application are difficult to obtain. The specifications include 0.5 mm range of motion, available force of at least 0.05 N, and maximum diameter of 6 mm. We have experimented with various actuators for the instrument, including voice coils and piezoceramic elements, but have found none completely satisfactory. We are currently working with NASA to obtain actuators made of a new high-displacement piezoceramic material called Thunder, currently being prepared for commercialization.

The present prototype is designed only for experiments in positioning of the tip. It has no end-effector. The final instrument prototype will incorporate an end-effector as described above, protruding from the intraocular shaft. Tip movement under the current manipulator design involves motion of the upper centroid, changing the distance between the upper and lower centroids. This means that the length of the inner shaft, running from the lower centroid to the upper, and then through the intraocular shaft to the tip, will change as the manipulator moves. The final prototype will therefore include a fourth actuator to change the length of the inner shaft as appropriate to maintain its position with respect to the tip of the intraocular shaft. Actuation of the end-effector in the final prototype will be accomplished using the RCA technique of Rader *et al*.[8], in order to avoid end-effector actuation artifacts.

3. CONTROL

In its present state, with 3-dof sensing, only irrotational experiments can be conducted with the instrument. Therefore the linear accelerations sensed can be straightforwardly integrated twice to obtain position signals for input to the control system. The future incorporation of 6-dof sensing and subsequent 6-dof experimentation will require determination of tip acceleration using the standard techniques of vector mechanics, and then, as here, double integration to obtain position.

The overall operation of the system is depicted in Figure 2. The uncompensated position of the instrument tip being obtained from the sensors, an error filter such as those described in §4 is implemented, producing an estimate in real time of the undesired component of the instrument motion. This estimate is then used as input to the controller of the tip manipulator, causing it to compensate the error by deflecting in opposition to it.

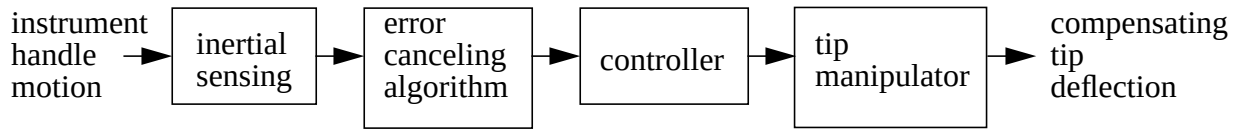

Figure 2. The error compensation system implemented by the active hand-held instrument. Inertial sensors measure the motion of the handle, from which the motion of the tip is derived. An error canceling algorithm performs real-time discrimination of the undesired component of motion, which is then input to the controller in order to generate a compensating instrument tip deflection via the manipulator.

To generate the desired compensating deflection obtained from the error filter, the controller must compute the inverse kinematics of the manipulator. This consists of determining the actuator lengths needed to reach a given tip position. We present the inverse kinematics here in a form amenable to online computation. Let vectors $\boldsymbol{n}$, $\boldsymbol{o}$, and $\boldsymbol{a}$ be the directional cosines of the frame *xyz* in the coordinates of the base frame ξψω. The orthonormality of $\boldsymbol{n}$, $\boldsymbol{o}$, and $\boldsymbol{a}$ leads to the following constraints[9]:

$$\boldsymbol{n}\cdot\boldsymbol{n}=1 \tag{1}$$
$$\boldsymbol{o}\cdot\boldsymbol{o}=1 \tag{2}$$
$$\boldsymbol{a}\cdot\boldsymbol{a}=1 \tag{3}$$
$$\boldsymbol{n}\cdot\boldsymbol{o}=0 \tag{4}$$
$$\boldsymbol{o}\cdot\boldsymbol{a}=0 \tag{5}$$
$$\boldsymbol{a}\cdot\boldsymbol{n}=0 \tag{6}$$

The displacement (d_x, d_y, d_z) of the intraocular probe tip is

$$d_x = x_c + la_1 \tag{7}$$
$$d_y = y_c + la_2 \tag{8}$$
$$d_z = z_c - z_{c_0} + l(a_3 - 1)\ . \tag{9}$$

The pin joints at the lower ends of the actuators impose the constraints[9]

$$n_2 = o_1 \tag{10}$$

$$X_c = \frac{\rho}{2}(n_1 - o_2) \tag{11}$$

$$n_2\rho + Y_c = 0\,. \tag{12}$$

where $X_c=x_c/R$, $Y_c=y_c/R$.

This system (1-12) must be solved to obtain the actuator lengths. The remaining equations in this section are the computations which must be carried out online. The system is first solved for the directional cosine o_2. To do so, it is necessary to root the following quartic equation:

$$A_{o2}\xi^4 + B_{o2}\xi^3 + C_{o2}\xi^2 + D_{o2}\xi + E_{o2} = 0\,, \tag{13}$$

where

$$A_{o2} = 8r^4l^2 + r^6 + 16r^2l^4 \tag{14}$$

$$B_{o2} = 20r^3d_xl^2 - 16r^2l^4 + 4r^5d_x - 4r^6 - 20r^4l^2 + 16rd_xl^4 \tag{15}$$

$$C_{o2} = 4d_x^2l^4 - 12r^5d_x - 12r^2l^4 - 2r^4d_y^2 + 8r^2d_x^2l^2 - 36r^3d_xl^2 + 4r^4d_x^2 + 4d_y^2l^4 + 20d_y^2l^2r^2 + 12r^4l^2 - 24rd_xl^4 + 6r^6 \tag{16}$$

$$D_{o2} = -8r^4d_x^2 - 8d_x^2l^4 + 20rd_y^2d_xl^2 + 8r^2l^4 + 12r^5d_x - 4r^3d_y^2d_x + 4r^4l^2 - 16r^2d_x^2l^2 - 4r^6 - 20d_y^2l^2r^2 + 12r^3d_xl^2 + 4r^4d_y^2 \tag{17}$$

$$E_{o2} = 4d_y^4l^2 + 4r^3d_y^2d_x - 4d_y^2l^4 - 2r^4d_y^2 - 20rd_y^2d_xl^2 - 4r^5d_x - 4r^4l^2 + r^6 + 4r^4d_x^2 + r^2d_y^4 + 4d_x^2l^4 + 8r^2d_x^2l^2 + 4r^3d_xl^2 + 8rd_xl^4 + 4r^2l^4 \tag{18}$$

This equation may be rooted via the resolvent cubic method[10], which involves rooting the cubic equation

$$\zeta^3 + b_{o2}\zeta^2 + c_{o2}\zeta + d_{o2} = 0 \tag{19}$$

where

$$b_{o2} = -2C_{o2} \tag{20}$$

$$c_{o2} = C_{o2}^2 + B_{o2}D_{o2} - 4A_{o2}E_{o2} \tag{21}$$

$$d_{o2} = -B_{o2}C_{o2}D_{o2} + B_{o2}^2E_{o2} + A_{o2}D_{o2}^2\,. \tag{22}$$

One root of this equation is needed, and it may be determined analytically as follows. Computing

$$v_{o2} = \sqrt[3]{-\frac{-9a_{o2}b_{o2}c_{o2} + 27a_{o2}^2d_{o2} + 2b_{o2}^3}{54a_{o2}^3} + \frac{\sqrt{3\left(4a_{o2}c_{o2}^3 - b_{o2}^2c_{o2}^2 - 18a_{o2}b_{o2}c_{o2}d_{o2} + 27a_{o2}^2d_{o2}^2 + 4b_{o2}^3d_{o2}\right)}}{18a_{o2}^2}}\,, \tag{23}$$

the root, u_{o2}, may then be calculated.

$$u_{o2} = v_{o2} + \frac{-3a_{o2}^2c_{o2}^2 + b_{o2}^2}{9a_{o2}^2v_{o2}} - \frac{b_{o2}}{3a_{o2}} \tag{24}$$

The resolvent cubic above is derived by factoring the quartic into two quadratic expressions[10]. Only one root is physically meaningful, and is found as follows:

$$G_{o2} = \frac{1}{2}\left(B_{o2} + \sqrt{B_{o2}^2 - 4A_{o2}u_{o2}}\right) \tag{25}$$

$$H_{o2} = \frac{C_{o2} - u_{o2}}{2} + \frac{B_{o2}(C_{o2} - u_{o2}) - 2A_{o2}D_{o2}}{2\sqrt{B_{o2}^2 - 4A_{o2}u_{o2}}} \tag{26}$$

$$o_2 = \frac{-G_{o2} + \sqrt{G_{o2}^2 - 4A_{o2}H_{o2}}}{2A_{o2}} \tag{27}$$

Having obtained o_2, we then calculate the remaining directional cosines. First, o_3 is calculated.

$$v_{o3} = -r^2 - 2rd_x + d_y^2 - 2o_2r^2 + 2o_2rd_x + 3o_2^2r^2 \tag{28}$$

$$o_3 = -\sqrt{\frac{v_{o3o}}{-2r^2 + l^2}} \tag{29}$$

The sign of o_1 is not known, but its square may be calculated using (2):

$$o_1^2 = 1 - o_2^2 - o_3^2. \tag{30}$$

Then, from (10),

$$n_2^2 = o_1^2. \tag{31}$$

A quadratic must be solved to obtain n_1.

$$a_{n1} = \frac{r^2}{4} + l^2 \tag{32}$$

$$b_{n1} = -rd_x - \frac{r^2 o_2}{2} \tag{33}$$

$$c_{n1} = d_x^2 + rd_x o_2 + \frac{1}{4} r^2 o_2^2 - l^2\left(o_1^2 + o_2^2\right) \tag{34}$$

The correct root is then

$$n_1 = \frac{-b_{n1} + \sqrt{b_{n1}^2 - 4a_{n1}c_{n1}}}{2a_{n1}}. \tag{35}$$

Then, from

$$a_1 = \frac{2d_x - rn_1 + ro_2}{2l} \tag{36}$$

$$a_3 = \sqrt{1 - a_1^2 - a_2^2} \tag{37}$$

$$n_3 = -\mathrm{sgn}\,(d_x)\sqrt{1 - o_3^2 - a_3^2} \tag{38}$$

$$n_2 = -\frac{n_3 o_3}{n_1 o_2} \tag{39}$$

The remaining directional cosines, o_1 and a_2, may now be calculated also, but are not needed, and are therefore omitted. To complete the inverse kinematics, the actuator lengths may now be computed as follows[9]:

$$\lambda_1 = R\sqrt{(n_1\rho + X_c - 1)^2 + (n_2\rho + Y_c)^2 + (n_3\rho + Z_c)^2} \tag{40}$$

$$\lambda_2 = \frac{R}{2}\sqrt{\left(-n_1\rho + \sqrt{3}o_1\rho + 2X_c + 1\right)^2 + \left(-n_2\rho + \sqrt{3}o_2\rho + 2Y_c - \sqrt{3}\right)^2 + \left(-n_3\rho + \sqrt{3}o_3\rho + 2Z_c\right)^2} \tag{41}$$

$$\lambda_3 = \frac{R}{2}\sqrt{\left(-n_1\rho - \sqrt{3}o_1\rho + 2X_c + 1\right)^2 + \left(-n_2\rho - \sqrt{3}o_2\rho + 2Y_c + \sqrt{3}\right)^2 + \left(-n_3\rho - \sqrt{3}o_3\rho + 2Z_c\right)^2}, \tag{42}$$

where $Z_c = z_c/R$.

4. PRELIMINARY EXPERIMENTS

Our work in error canceling algorithms for improved precision in microsurgery has involved the development of adaptive filtering and neural network algorithms for real-time compensation of tremor and low-frequency error. These algorithms have been demonstrated with a 1-dof instrument and in simulation. The algorithms described below will be implemented in the present instrument prototype.

4.1. Tremor canceling

In ophthalmological microsurgery, the rms amplitude of physiological tremor ranges from approximately 5 to 50 μm[5,8]. We have demonstrated active canceling of tremor using an early instrument prototype with one degree of freedom[11]. This instrument used flexure of the intraocular shaft to perform compensation in one dimension transverse to the shaft. The flexure was induced by a pair of piezoelectric elements mounted on opposite sides of the shaft at its base. The motion of the tip, rather than of the handle as in the current instrument, was measured using a non-contact Hall effect sensor.

Taking the place of the surgeon's hand was a voice coil actuator that provided 1-D input motion to the instrument, moving the base of the cantilever shaft or beam up and down. Input data for the voice coil were recorded from ophthalmological surgeons in a practice surgical suite[8]. Surgeons attempted to hold an instrument motionless within an artificial eye for 16 s, while a Hall effect sensor measured the position of a 0.26 g magnet mounted on the instrument tip.

Estimation of tremor was performed by a system based on the weighted-frequency Fourier linear combiner (WFLC) algorithm[12]. The WFLC is an adaptive algorithm that estimates tremor using a sinusoidal model, estimating its time-varying frequency, amplitude, and phase. It is an extension of the Fourier linear combiner (FLC), which adaptively estimates amplitude and phase given a fixed fundamental frequency[13]. To cancel tremor in a microsurgical instrument, a parallel arrangement of the WFLC and FLC was used. The WFLC operated with bandpass prefiltering, to minimize frequency estimation errors due to non-tremor motion. Its tremor frequency information was then used as the reference for a FLC, with no prefiltering, which provided real-time amplitude and phase estimation and tremor modeling, without time delay. The bandpass prefiltering phase lag therefore affected only the frequency estimation, which was already constrained to adapt only slowly for stability, and had no effect on the amplitude and phase adaptation. Recordings of hand motion were fed through the test apparatus, both with and without tremor compensation. Figure 3 shows the results of a typical experiment. The dashed line indicates recorded hand motion, fed through the instrument via the voice coil, without compensation. This dashed line offers a view of the general appearance of hand motion, in which both tremor and lower-frequency components may easily be distinguished. The solid line represents the results of active compensation with the same input signal. Tests

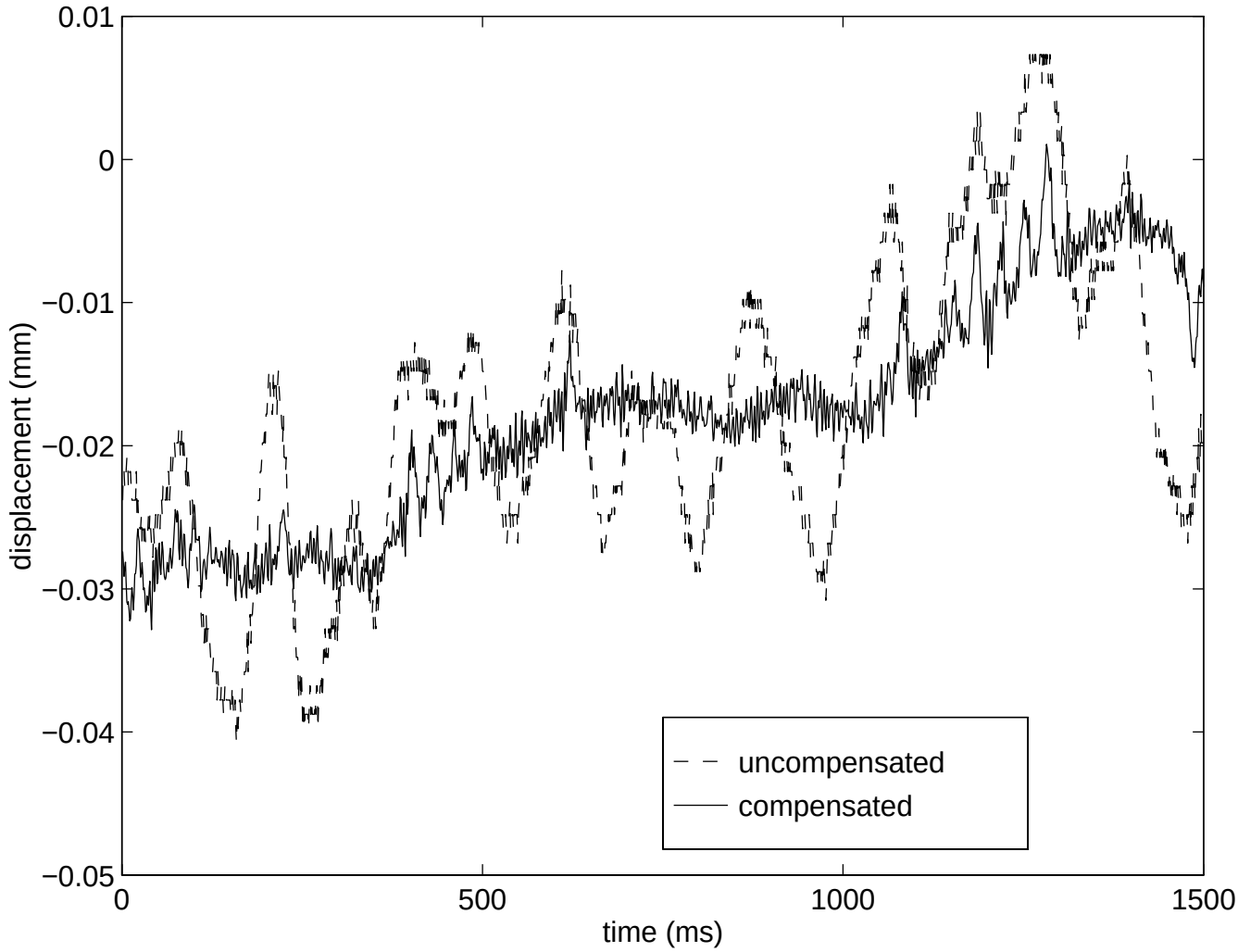

Figure 3. Results of canceling physiological hand tremor in 1-D instrument. The dashed line represents the uncompensated motion, generated by feeding recorded hand motion through the instrument without tremor compensation. The solid line represents the same input motion, this time with the tremor compensation operating.

of this technique demonstrated rms amplitude reduction of more than 60% in the 6-16 Hz tremor band, and rms error reduction of over 20% with respect to an offline estimate of non-tremor motion[11].

4.2. Low-frequency error canceling

Measurements of the hand motion of surgeons have shown the presence of low-frequency error, or drift, when attempting to hold an instrument at a fixed target[2]. The 0.5 mm range of motion of the active instrument is designed to allow canceling of low-frequency error in microsurgery. We have demonstrated, in simulations, the feasibility of compensating this type of position error[14]. As in the previous experiment, 1-D data were recorded from surgeons attempting to hold an instrument motionless within an artificial eye in a practice surgical suite[8]. Data were sampled at 250 Hz. Since the target in these tests was stationary, any motion is considered to be error.

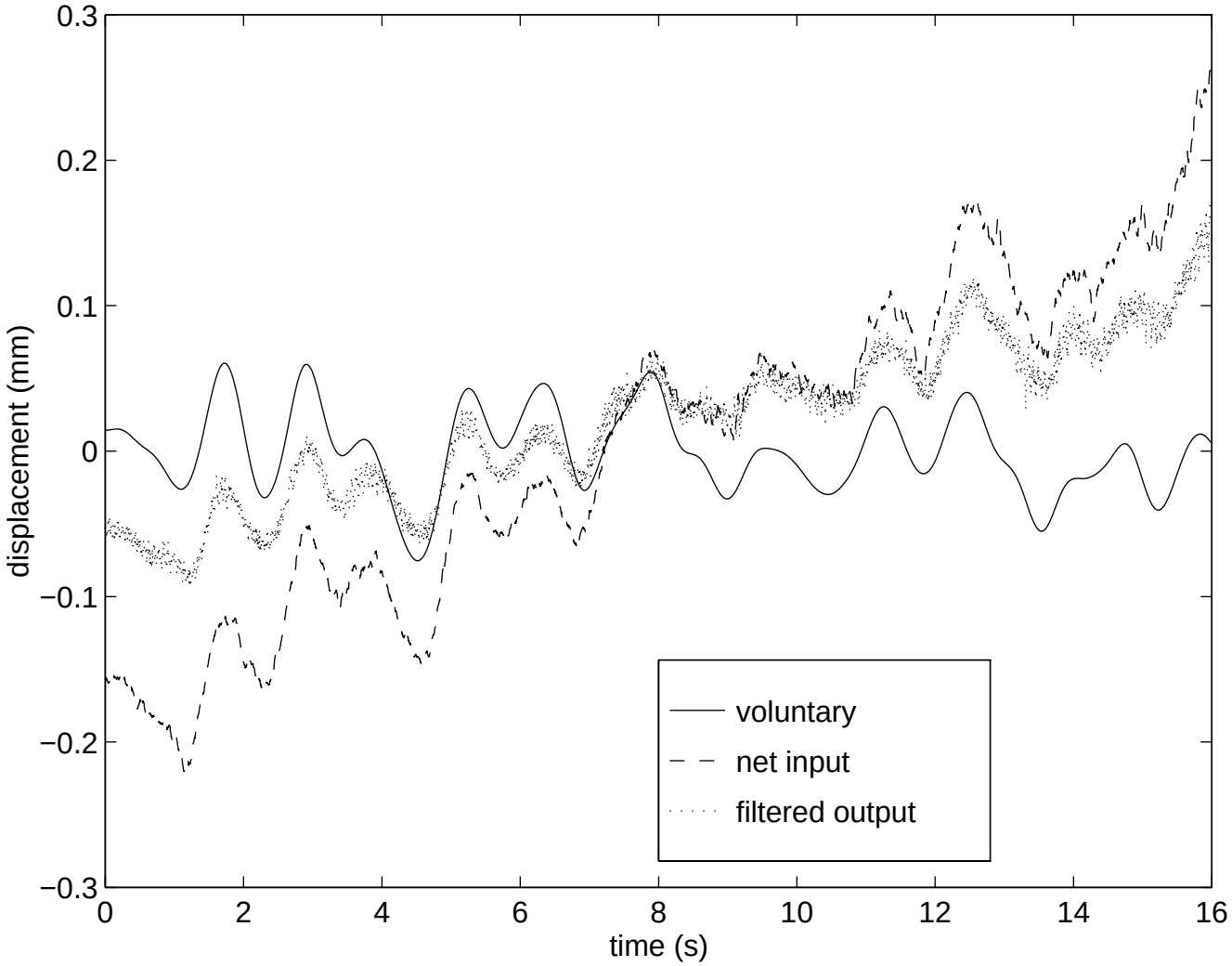

Figure 4. Results from canceling of low-frequency error. The solid line shows the pseudo-voluntary motion, generated by lowpass filtering white noise at 1 Hz cutoff frequency. The dashed line represents the neural network input for the test, obtained by adding recorded hand motion error to the pseudo-voluntary motion. The dotted line indicates the filtered version of the data, obtained by subtracting the neural network estimate of the position error from the input signal. The filtered output thus represents a simulation of the result of compensation of low-frequency error during microsurgery with the active hand-held instrument.

Less is known about low-frequency error in small-scale manipulation than about physiological tremor. Discriminating low-frequency error is particularly difficult because its frequency band is the same as that of voluntary motion. To distinguish between these two largely unknown signal components, a cascade neural network[15] was used, due to its versatility in learning unknown dynamics[16]. The cascade learning architecture allows the neural network to adjust not only the values of network weights, but also the number of hidden units and the transfer functions of those units. The network starts with no hidden nodes, then adds them one by one as error performance stagnates, as determined by a preselected threshold. With each new hidden node, several candidate transfer functions are implemented in parallel, including sigmoids, Bessel functions, and sinusoids, and the one with best performance is selected after a brief period of comparison. Extended Kalman filtering is used for learning, having been found superior in performance to backpropagation[17].

After training, the network used here had 100 input nodes in a tapped delay line structure, 10 hidden nodes, and one output node. Given an input containing both desired and undesired motion, the network estimated the undesired component, which would serve as a command to a compensating actuator. In the simulation, this output was then subtracted from the input to obtain an estimate of the desired or voluntary input component. The signal used as voluntary motion in this simulation was a pseudo-voluntary signal generated by lowpass filtering white noise with a 1 Hz cutoff frequency. Figure 4 shows the results of a typical experiment. The solid line shows the pseudo-voluntary motion. The dashed line represents the input to the neural network, consisting of the sum of the pseudo-voluntary motion and recorded hand motion error obtained as described above. The filtered output obtained by subtracting the neural network output from the input, is indicated by the dotted line. These tests have resulted in an average reduction of rms error of over 40% with respect to the pseudo-voluntary motion[14].

5. DISCUSSION

The research effort described here aims toward significant improvement of the precision of the surgeon in micromanipulation, by canceling tremor and other types of position error in a hand-held instrument that is essentially identical in look and feel to existing instruments. Rather than replacing the human hand, which is already a very capable manipulator, it aims to retain the benefits of the human system, and merely augment it to the degree necessary to attain the goal of 10 μm precision[4] in ophthalmological microsurgery. This holds the promise not only of improving current procedures, but also of enabling entirely new procedures that have thus far been impossible due to the limited available precision[4].

The aim of the current prototype is to incorporate sensing and actuation, with precision of 5 μm or better, within a realistic size and shape for a hand-held ophthalmological microsurgical instrument. MEMS technology has allowed the size constraint on sensors to be met by both the present accelerometers and the rate gyros that will be incorporated in the future. The new Thunder actuators from NASA appear to strike the right balance in the familiar tradeoff between range of motion and available force. The final prototype will focus on the integration of end-effectors and the remote cam actuation scheme with the other components of the active instrument. This will include an additional actuator to change the length of the inner tool-bearing shaft in order to maintain proper positioning of the end-effector with respect to the tip of the outer intraocular shaft.

The experiments with the 1-dof instrument and the simulations demonstrate the feasibility of suppressing both physiological tremor and other types of error in microsurgery using hand-held instruments and an active compensation approach. Error compensation experiments with the present prototype will involve canceling of both tremor and non-tremor errors in laboratory experiments, with the instrument mounted on a high-precision robotic manipulator, acting as the "surgeon's hand." These trials will continue with the 6-dof instrument when it becomes available. Evaluation of the final prototype will then proceed to human subject tests of the instrument, performing simulated surgical tasks with and without active compensation.

Further research will include the exploration of possibilities for extension of the technology into other microsurgical fields where improved manual precision is needed, including neurosurgical, otological, and microvascular surgery[4]. Adaptation to these fields will consist primarily of modifications in the geometry of the instrument[4]. Low-frequency error will also be studied further. Whereas physiological tremor is definitely involuntary, it is not yet clear to what extent the low-frequency error, which is certainly undesirable, is strictly due to involuntary processes. Future investigation will also involve examination of the effect on canceling performance of closing the loop via the surgeon's vision.

6. CONCLUSION

The ongoing development of an active hand-held instrument for compensation of position error in ophthalmological microsurgery has been summarized. The design of the manipulator that deflects the instrument tip for error canceling has been presented, including a formulation of the inverse kinematics in a tractable manner for online computation within the control system. Demonstrations of the feasibility of active canceling of hand tremor and other errors, both by experimentation with a 1-dof instrument and by simulation, have been reviewed.

ACKNOWLEDGMENTS

Funding provided by Defense Advanced Research Projects Agency (DARPA). The authors are grateful to H. Benjamin Brown for design advice., and to Dr. R. Scott Rader for assistance with data acquisition.

REFERENCES

1. R. J. Elble and W. C. Koller, *Tremor*, p. 1, Johns Hopkins University Press, Baltimore, 1990.
2. C. N. Riviere, R. S. Rader, and P. K. Khosla, "Characteristics of hand motion of eye surgeons," *Proc. 19th Intl. Conf. IEEE Eng. Med. Biol. Soc.*, to appear, 1997.
3. P. S. Schenker, E. C. Barlow, C. D. Boswell, H. Das, S. Lee, T. R. Ohm, E. D. Paljug, G. Rodriguez, and S. T. Charles, "Development of a telemanipulator for dexterity enhanced microsurgery," *Proc. 2nd Intl. Symp. Med. Robot. Comput. Assist. Surg.*, pp. 81-88, 1995.
4. S. Charles, "Dexterity enhancement for surgery," *Computer Integrated Surgery: Technology and Clinical Applications*, R. H. Taylor, S. Lavallée, G. C. Burdea, and R. Mösges, eds., pp. 467-471, MIT Press, Cambridge, 1996.
5. I. W. Hunter, T. D. Tilemachos, S. R. Lafontaine, P. G. Charette, L. A. Jones, M. A. Sagar, G. D. Mallinson, and P. J. Hunter, "A teleoperated microsurgical robot and associated virtual environment for eye surgery," *Presence*, vol. 2, pp. 265-280, Fall 1993.
6. R. H. Taylor, S. Lavallée, G. C. Burdea, and R. Mösges (eds.), *Computer Integrated Surgery: Technology and Clinical Applications*, p. 465, MIT Press, Cambridge, 1996.
7. H. N. Jacobus, A. J. Riggs, C. J. Jacobus, and Y. Weinstein, "Implementation issues for telerobotic handcontrollers: human-robot ergonomics," *Human-Robot Interaction*, M. Rahimi and W. Karwowski, eds., pp. 284-314, Taylor and Francis, London, 1992.
8. Rader, R. S., Walsh, A. C., Awh, C. C., and de Juan, E., Jr., "Manual stability analysis of vitreoretinal microsurgery tasks," *Ergonomics*, in review, 1997.
9. K.-M. Lee and D. K. Shah, "Kinematic analysis of a three-degrees-of-freedom in-parallel actuated manipulator," *IEEE Trans. Robot. Autom.*, vol. 4, pp. 354-360, June 1988.
10. S. Neumark, *Solution of Cubic and Quartic Equations*, ch. 3, Pergamon, Oxford, 1965.
11. C. N. Riviere, R. S. Rader, and N. V. Thakor, "Adaptive canceling of physiological tremor for improved precision in microsurgery," *IEEE Trans. Biomed. Eng.*, to appear, 1997.
12. C. N. Riviere and X. Kong, "The weighted-frequency Fourier linear combiner," *IEEE Trans. Signal Process.*, in review, 1997.
13. C. A. Vaz, X. Kong, and N. V. Thakor, "An adaptive estimation of periodic signals using a Fourier linear combiner," *IEEE Trans. Signal Process.*, vol. 42, pp. 1-10, 1994.
14. C. N. Riviere and P. K. Khosla, "Augmenting the human-machine interface: improving manual accuracy," *Proc. IEEE Intl. Conf. Robot. Autom.*, 1997. (Note: Results reported as mm are actually inches.)
15. S. E. Fahlman and C. Lebiere, "The cascade-correlation learning algorithm," in D. S. Touretzky, ed., *Advances in Neural Information Processing Systems 2*, Los Altos, Ca.: Morgan Kauffman, pp. 524-532, 1990.
16. M. Nechyba, and Y. Xu, "Human skill transfer: neural networks as learners and teachers," *Proc. IEEE Intl. Conf. Intell. Robots Syst.*, vol. 3, pp. 314-319, 1995.
17. G. V. Puskorius and L. A. Feldkamp, "Decoupled extended Kalman filter training of feedforward layered networks," *Proc. Intl. Joint Conf. Neural Networks*, vol. 1, pp. 771-777, 1991.